microbial biotechnology

Microbial Biotechnology (2010) **3**(1), 93–106 doi:10.1111/j.1751-7915.2009.00154.x

Pleurotus ostreatus manganese-dependent peroxidase silencing impairs decolourization of Orange II

Tomer M. Salame, Oded Yarden and Yitzhak Hadar*
Department of Plant Pathology and Microbiology, The Robert H. Smith Faculty of Agriculture, Food and Environment, The Hebrew University of Jerusalem, Rehovot 76100, Israel.

Summary

Decolourization of azo dyes by *Pleurotus ostreatus*, a white-rot fungus capable of lignin depolymerization and mineralization, is related to the ligninolytic activity of enzymes produced by this fungus. The capacity of *P. ostreatus* to decolourize the azo dye Orange II (OII) was dependent and positively co-linear to Mn^{2+} concentration in the medium, and thus attributed to Mn^{2+}-dependent peroxidase (MnP) activity. Based on the ongoing *P. ostreatus* genome deciphering project we identified at least nine genes encoding for MnP gene family members (*mnp1–9*), of which only four (*mnp1–4*) were previously known. Relative real-time PCR quantification analysis confirmed that all the nine genes are transcribed, and that Mn^{2+} amendment results in a drastic increase in the transcript levels of the predominantly expressed MnP genes (*mnp3* and *mnp9*), while decreasing versatile peroxidase gene transcription (*mnp4*). A reverse genetics strategy based on silencing the *P. ostreatus mnp3* gene by RNAi was implemented. Knock-down of *mnp3* resulted in the reduction of fungal OII decolourization capacity, which was co-linear with marked silencing of the Mn^{2+}-dependent peroxidase genes *mnp3* and *mnp9*. This is the first direct genetic proof of an association between MnP gene expression levels and azo dye decolourization capacity in *P. ostreatus*, which may have significant implication on understanding the mechanisms governing lignin biodegradation. Moreover, this study has proven the applicability of RNAi as a tool for gene function studies in *Pleurotus* research.

Introduction

Pleurotus ostreatus is a commercially important edible white-rot basidiomycete known as the oyster mushroom. The ligninolytic system of *Pleurotus* species has been found to be mainly composed of the lignin-modifying enzymes (LMEs) laccase, aryl-alcohol oxidase and two types of peroxidases: Mn^{2+}-dependent peroxidase (MnP) and versatile peroxidase (VP). All of these enzymes may function separately or in cooperation (Cohen *et al.*, 2002a; Stajić *et al.*, 2009). Versatile peroxidase has been suggested to be a MnP-LiP (lignin peroxidase) 'hybrid', based on its ability to oxidize different substrates in the presence or the absence of Mn^{2+}, its crystal structure and theoretical molecular models (Camarero *et al.*, 1999; Ruiz-Dueñas *et al.*, 2001; Martínez, 2002). In recent years, different Mn^{2+} peroxidases, designated MnP1–4, have been purified and characterized from *Pleurotus* species and their corresponding genes (*mnp1–4*) were sequenced and analysed (Asada *et al.*, 1995; Ruiz-Dueñas *et al.*, 1999; Giardina *et al.*, 2000; Irie *et al.*, 2000). The peroxidases MnP1, MnP2 and MnP4 were characterized as VPs while MnP3 was characterized as a MnP (Cohen *et al.*, 2001).

Manganese peroxidases are the most common ligninolytic peroxidases produced by almost all white-rot basidiomycetes and by various litter-decomposing fungi. The remarkable degradative potential of MnP makes this enzyme an attractive versatile biocatalyst for biotechnological and environmental applications, e.g. in pulping and bleaching of lignocellulose, in removing of hazardous wastes or in certain organic syntheses (Hofrichter, 2002; Cohen *et al.*, 2002a; Hammel and Cullen, 2008; Stajić *et al.*, 2009). Effective harnessing of these applications is dependent on establishing a comprehensive understanding of the enzyme's properties and mode of action. The ability of lignin-degrading white-rot fungi (WRF) to degrade a wide range of synthetic chemicals, including dyes (many of which are recalcitrant to biodegradation) has been reported and linked to the ligninolytic process, i.e. the activity of LMEs that take part in the lignin depolymerization process, which is non-specific in nature. These enzymes play significant roles in dye metabolism due to the structural similarity of most commercially relevant dyes to lignin (sub)structures amenable to be transformed by LMEs. So far, WRF have been found to be the most efficient microorganisms in degrading synthetic dyes, and thus are currently being investigated in the development of bioremediation solutions for these polluting xenobiotics (Wesenberg *et al.*,

Received 13 August, 2009; revised 18 September, 2009; accepted 21 September, 2009. *For correspondence. E-mail hadar@agri.huji.ac.il; Tel. (+972) 8948 9935; Fax (+972) 8946 8785.

2003; Asgher *et al*., 2008; Faraco *et al*., 2009). Additionally, on the basis of the accumulated evidence, several methods involving dyes have been reported as screening methodologies for investigation of the ligninolytic process. The use of dyes offers a number of advantages over conventional natural substrates because they are stable, soluble and affordable with high molar extinction rates and low toxicity. These dyes can be applied in simple, quick and quantitative spectrophotometric assays, thereby serving as a basis for simple phenotypic-based assays for the functionality of the ligninolytic system (Glenn and Gold, 1983; Platt *et al*., 1985; Field *et al*., 1993; Shrivastava *et al*., 2005; Hernández-Luna *et al*., 2008; Lucas *et al*., 2008). In this study, the azo dye Orange II (OII) was chosen as a model compound because it is a representative of a large class of extensively used commercial dyes, and its complex structure presents several characteristics (such as its aromatic structure, azo linkage and a sulfonic group) that are relevant to many xenobiotics and contaminants. This dye was previously shown to be decolourized by *P. ostreatus* (Knapp *et al*., 1995). Moreover, its decolourization by the white-rot basidiomycetes strain F29 (Knapp *et al*., 1997) and *Bjerkandera* sp. (Mielgo *et al*., 2003; López *et al*., 2004) was found to be positively affected by Mn^{2+} amendments, which may suggest the involvement of Mn^{2+} peroxidases. Decolourization of OII servers as a measure of its degradation, as a higher UV-VIS absorbance correlates with a higher dye concentration (Mielgo *et al*., 2001; 2003).

Mn^{2+} ions are naturally present in wood and lignocellulose residues. Several studies have shown the effect of Mn^{2+} on enhancing lignin degradation and mineralization by *Pleurotus* species, suggesting the importance of MnP in the process (Camarero *et al*., 1996; Kerem and Hadar, 1997; Cohen *et al*., 2001; 2002b). Cohen and colleagues (2001) used semi-quantitative RT-PCR to monitor the relative expression levels of the four *mnp* genes as affected by Mn^{2+} amendment. That study described a reduction in the abundance of VP genes transcript and an increase in *mnp3* transcript, which were co-linear with the changes observed in the MnP enzymes' activity profiles. These results have indicated the importance of MnP in lignin degradation and that transcriptional regulation plays a role in the process. Nevertheless, most of the information regarding the significance of Mn^{2+}-dependent peroxidase in this process has been derived from hypotheses based on indirect findings.

The feasibility of affecting gene expression in *P. ostreatus* by genetic manipulation is an invaluable tool for the dissection of the LMEs functionality in this fungus. Honda and colleagues (2000) developed a PEG-$CaCl_2$-meditated method for transformation and recombinant gene expression system in *P. ostreatus*, based on the homologous drug-resistant marker gene *Cbx*^{R}, which confers dominant resistance to the systemic fungicide carboxin. This system has since been used for the homologous expression of recombinant Mn^{2+} peroxidase genes (Irie *et al*., 2001a; Tsukihara *et al*., 2006). However, homologous recombination has been shown to occur only rarely, rendering gene knockout studies difficult (Honda *et al*., 2000; Irie *et al*., 2001a).

RNA interference (RNAi) is a post-transcriptional gene-silencing phenomenon in which double-stranded RNA (dsRNA) triggers the degradation of homologous mRNA, thereby diminishing or abolishing gene expression. Three fundamental components of the RNA silencing machinery have been identified: Argonaute, Dicer and RNA-dependent RNA polymerase (RdRP) (Tomari and Zamore, 2005; Nakayashiki *et al*., 2006; Nakayashiki and Nguyen, 2008). These have been identified in a wide range of fungi including ascomycetes, basidiomycetyes and zygomycetes, many of which harbour multiple RNA silencing components in the genome, whereas a portion of ascomycete and basidiomycete fungi apparently lacks most of or whole of the components. In addition to being recognized as a principal mechanism for controlling eukaryotic gene expression, the natural occurrence of this phenomenon has also been harnessed as a tool for elucidating gene function. As an efficient reverse genetics approach this technique involves the introduction or production of dsRNA molecules homologous to the gene being targeted for silencing in the cell of interest. RNAi has been proven effective in most eukaryotes, including vertebrates, plants, invertebrates, protists and fungi (Nakayashiki *et al*., 2006; Nakayashiki and Nguyen, 2008).

The *P. ostreatus* (monokaryon PC15) genome sequencing project has been recently completed by the DOE JGI (http://genome.jgi-psf.org/PleosPC15-1). The availability of the genome sequence, and the fact that the fungus is amenable to genetic modifications makes *P. ostreatus* accessible for comprehensive functional genomics studies. This has prompted us to study the involvement of MnPs in the degradation of aromatic substrates, using available and modified tools for gene manipulation in this fungus. To do so we facilitated a reverse genetics strategy of silencing the *P. ostreatus mnp3* gene using an RNAi-based approach, in combination with a comprehensive analysis of the expression levels of MnP gene family members. Consequently, we determined the effects of silencing *mnp3* on fungal growth, levels of MnP gene family expression in response to Mn^{2+} amendment, and the significance of Mn^{2+}-dependent peroxidases for the functionality of *P. ostreatus* ligninolytic system as evaluated by OII decolourization.

Results

Orange II decolourization is Mn^{2+} dependent

The capacity of the white-rot fungus *P. ostreatus* strain PC9 to decolourize OII was evaluated both on solid media and in liquid culture, in the presence of Mn^{2+} at several concentrations ranging 0–270 μM. Mn^{2+} concentration in the non-amended medium was determined by atomic absorption spectroscopy and was found to be less than 0.1 μM. On solid medium, linear growth rate was not affected by the Mn^{2+} amendments, yet decolourization was apparent only at concentrations above 8.1 μM, and its intensity was increased with elevation of Mn^{2+} concentration in the medium (Fig. 1A). In the absence of Mn^{2+} no visible changes in OII colour intensity were observed even after 30 days of incubation. Media containing Mn^{2+} concentrations higher than 54 μM showed formation of dark precipitation foci of MnO_2 (López *et al*., 2007). Consequently, for further analysis on solid media we used Mn^{2+} at a concentration of 27 μM. Decolourization was also monitored in liquid culture for 10 days (Fig. 1B), showing a similar dependency on Mn^{2+} concentration. The fungal dry weight in liquid culture was similar in all treatments (average of 256 mg/flask after 10 days of incubation, with a ±4% deviation). OII decolourization did not occur in non-inoculated media, at any of the examined Mn^{2+} concentrations, even after 30 days of incubation. Since this reaction depends on the presence of Mn^{2+} and there was no decolourization in the absence of Mn^{2+}, it was attributed to Mn^{2+}-dependent peroxidase activity. Accordingly, OII decolourization can serve as a differential phenotypic assay for the expression level of these enzymes and was used here to assess *mnp3* silenced strains.

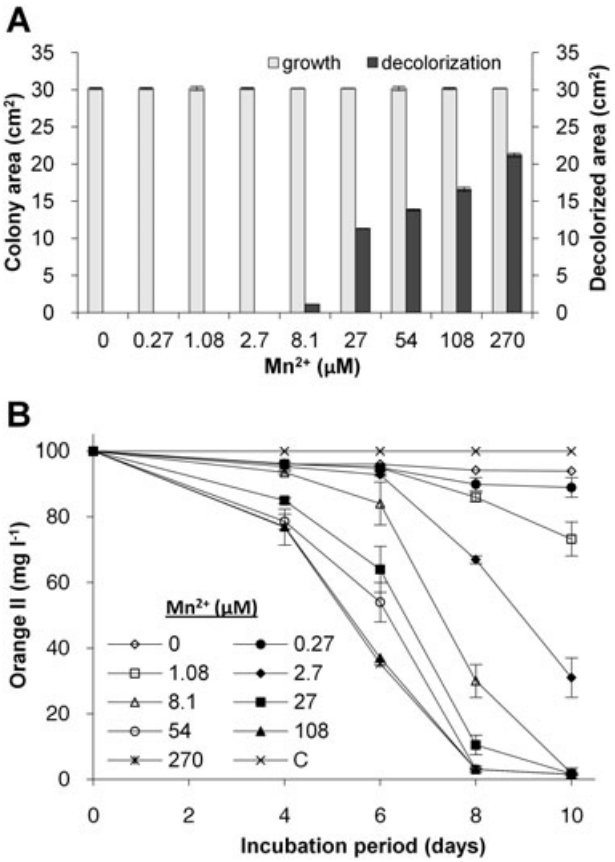

Fig. 1. A. Orange II decolourization by *P. ostreatus* PC9 grown on solid GP culture media containing several concentrations of Mn^{2+} (0–270 μM), after 10 days of incubation. The light and dark columns represent mycelial growth and decolourized areas respectively. Data represent the average of three biological replicates. Bars denote the standard deviation.
B. Time-course assay of Orange II decolourization by *P. ostreatus* PC9 in liquid GP media, containing several concentrations of Mn^{2+} (0–270 μM), during 10 days of incubation. Curve *C* is a control consisting of non-inoculated media. Data represent the average of three biological replicates. Bars denote the standard deviation.

P. ostreatus harbours more than one Mn^{2+}-dependent peroxidase

The *P. ostreatus* genome sequencing project has revealed the existence of at least nine non-allelic genes coding for MnP gene family members (Table 1; http://genome.jgi-psf.org/PleosPC15-1). To date, only four of these genes (*mnp1–4*) have been studied (Cohen *et al*., 2001; 2002b). Of these known genes, only *mnp3* encodes a Mn^{2+}-dependent peroxidase, whereas the others encode VPs (Mn^{2+}-independent peroxidases). We designated the additional five genes *mnp5–9* (Table 1). The deduced protein sequences of *mnp5–9* indicate that MnP6, 7, 8 and 9 are Mn^{2+}-dependent peroxidases, whereas MnP5 is most likely a VP (Asada *et al*., 1995; Ruiz-Dueñas *et al*., 1999; Giardina *et al*., 2000; Irie *et al*., 2000; Cohen *et al*., 2001). In order to study the effect of Mn^{2+} on the transcription profile of *P. ostreatus* MnP gene family members we used relative real-time PCR quantification analysis. The fungus was grown for 7 days in either a liquid medium amended with 27 μM Mn^{2+} (+Mn treatment) or a non-amended medium (–Mn treatment). The results presented in Fig. 2 show the relative expression of the nine different MnP gene family members. The primers used for real-time PCR analyses (Table 1) were verified to be gene-specific, and examination of melting curves indicated highly specific amplification of the respective cDNAs (data not shown). The endogenous control gene used was β-tubulin, and the calibrator was the –Mn treatment. Transcripts of all the nine *mnp* genes were detected in both Mn^{2+}-amended and non-amended cultures. However, Mn^{2+} in the medium affected the transcript abundance level of the *mnp* genes analysed in different manners. The transcripts levels of *mnp3* and *mnp9* were about 200-fold higher when Mn^{2+} was present in the medium; conversely, *mnp4* transcript abundance was about 70-fold higher in the non-amended medium.

Table 1. Sequences of oligonucleotides used in this study.

Gene	Primer designation	Sequence (5′→3′)[a]	bp	Expected amplicon (bp) DNA	Expected amplicon (bp) RNA	Reference[b]
pTMS1 silencing vector construction						
mnp3	MnP3C1	ATGGCCTTCAAGCACTTCT	19	–	1074	This study; GenBank FJ594281
	MnP3C2	TTATGAAGGGGGGACAGG	18			
sdi1	sdi1PF	GCATCCGCGGTCCGATGACACTGCCAAC	28	1324	–	Irie *et al.* (1998b)
	sdi1PR	CGTAGCTAGCGGTTCAATGATTTGTGTGTTCC	32			
mnp3	MnP3CAS750	CGATGCTAGCTCCAGCAAGAGGCGATTC	28	–	772	This study; GenBank FJ594281
	MnP3CAS1	CGTAGGCGCGCCATGGCCTTCAAGCACTTCTC	32			
mnp3	MnP3CS101	CGTAGGCGCGCCTACTGCGAACGCCGC	27	–	671	This study; GenBank FJ594281
	MnP3CS750	GCATACCGGTTCCAGCAAGAGGCGATTC	28			
sdi1	sdi1TF	CGTAACCGGTACACAAGTTAACGGCCACG	29	209	–	Irie *et al.* (1998a); GenBank FJ598647
	sdi1TR	CGTAGCATGCAGCATCGCAAGTGAAACC	28			
Analysis of construct integration						
sdi1 (*Cbx*^{R})	R1	CACACAAATCATTGAACC	18	1265	–	Honda *et al.* (2000)
	R3	AGCATCGCAAGTGAAACCGA	20			
pTMS1	pTMS1F3628	GTACGATTGGCGCAAAGATT	20	582	–	This study; pTMS1 silencing vector
	pTMS1R4191	GACACCGTCACCGATATCCT	20			
Real-time PCR						
β-tubulin	tubF543	GTGCGTAAGGAAGCTGAGGG	20	–	201	Cohen *et al.* (2001); JGI – Genome protein ID 16119
	tubR777	TGTGGCATTGTACGGCTCAAC	21			
mnp1	MnP1F1334	GTTCGCTCGAGACGATAGGACAT	23	–	187	Asada *et al.* (1995); JGI – Genome protein ID 166789
	MnP1R1619	GGGGAGATGTGGTTTGGTTACA	22			
mnp2	MnP2F737	GCCTTTCGATAGCGTGGATAAG	22	–	199	Giardina *et al.* (2000); JGI – Genome protein ID 30694
	MnP2R1123	GGTCCCTTGCAACATTGTCTC	21			
mnp3	MnP3F30	CCTCCTGACTTTGGCATCTCA	21	–	230	This study; GenBank FJ594281; JGI – Genome protein ID 185959
	MnP3R240	CACCTCCTCCACCTTTGGTT	20			
mnp4	MnP4F1269	TTGTTGGCTAGAGACCCCCAGA	22	–	186	Ruiz-Dueñas *et al.* (1999); JGI – Genome protein ID 186006
	MnP4R1609	CAAGTGGGCCGCTCCGAC	18			
mnp5	MnP5F52	CAGGCCGTCAATGCCGTA	18	–	237	JGI – Genome protein ID 156336
	MnP5R433	CGTAAGGACGGAACCATCA	19			
mnp6	MnP6F1133	TTCCCAGGTACTGCCGGA	18	–	181	JGI – Genome protein ID 168144
	MnP6R1515	CCAAAGACAGTTTCAACATCGC	22			
mnp7	MnP7F1293	CTTCATCTCCAACCCCAACTC	21	–	192	JGI – Genome protein ID 153232
	MnP7R1519	GCTTTGCGGCAGGATG	16			
mnp8	MnP8F1091	CTTCGACTCTACTCCCAACAGC	22	–	204	JGI – Genome protein ID 29594
	MnP8R1335	GAGGCGTGGTCGGTGAT	17			
mnp9	MnP9F1359	ATTGCTAATGAAAGGCTCATGGTT	24	–	192	JGI – Genome protein ID 23172
	MnP9R1588	GGTGGCAGCACAAGCAG	17			

a. Restriction sites are underlined.

b. In the case of data bank entries, GenBank and JGI *P. ostreatus* genome database are followed with accession numbers and protein ID numbers respectively. Note: referenced is the source of the primary sequences, all sequences were compared with JGI genome database which served as basis for primers design.

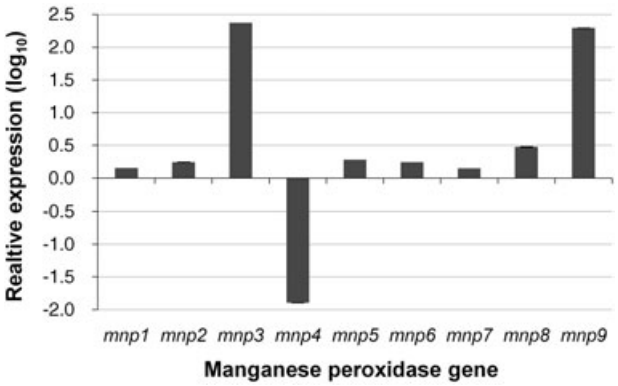

Fig. 2. Relative transcript abundance of *P. ostreatus* PC9 MnP gene family members in RNA extracted from a 7-day-old liquid culture in GP medium amended with 27 μM Mn^{2+} (+Mn treatment), relative to that measured in a non-amended medium (–Mn treatment), which served as the calibrator treatment. The expression of *mnp1–9* gene transcript abundance, relative to β-tubulin transcript abundance (endogenous control), was measured by real-time PCR relative quantification analysis using the ΔΔCT method. Data represent the average of three biological replicates. Bars denote the standard deviation; when not visible, the standard deviation is included within the graph line width. Note the log_{10} scale.

The transcript levels of all the other genes were increased by only 1.4- to 3-fold in the presence of Mn^{2+}, and were therefore not considered to be substantially induced. In addition, absolute quantification of the basal expression levels of the MnP gene family members, based on evaluation deduced from the real-time PCR amplification plots, indicate that, relative to the treatment, the transcript levels of *mnp3*, *4* and *9* were at least eightfold higher than those of the other *mnp* genes. Similar results were observed on the basis of semi-quantitative RT-PCR. The abundance of the β-tubulin transcript was not affected by the presence of Mn^{2+}. We therefore concluded that the presence of Mn^{2+} can affect different *mnp* genes in opposing ways.

Orange II decolourization capacity is inhibited in strains harbouring mnp3 RNAi constructs

To study the effect of reduced Mn^{2+}-dependent peroxidases gene expression, we transformed *P. ostreatus* with pTMS1, a construct designed to induce RNAi-based gene silencing of *mnp3*. Construct design was initially based on *mnp3*, a gene that was later found to be highly similar to *mnp9* in terms of Mn^{2+}-dependent gene regulation. pTMS1 (Fig. 3) was designed to express a single-stranded RNA that forms a loop (linker region), corresponding to basepairs 100–1 of the *mnp3* cDNA antisense strand, with a double-stranded stem, corresponding to basepairs 750–101 of the *mnp3* cDNA antisense, annealed to basepairs 101–750 of the *mnp3* sense strand. Formation of a hairpin RNA (hpRNA) structure, including the inverted repeat stem with a strong dsRNA secondary structure (a single 650-bp-long double-stranded stem in which the free energy of the structure is –1315.3 kkal mol^{-1}) was verified by RNA secondary structure prediction tools (http://www.genebee.msu.su/genebee.html).

The modified transformation procedure developed during the course of this study proved to be efficient and reproducible, yielding over 20 transformants per μg vector DNA; occurrence of abortive transformants was rare.

Thirty pTMS1 transformants were isolated, alongside one randomly chosen control strain (TC3) transformed with pTM1 (Honda *et al.*, 2000). All the transformants were grown in the presence of carboxin, and were found

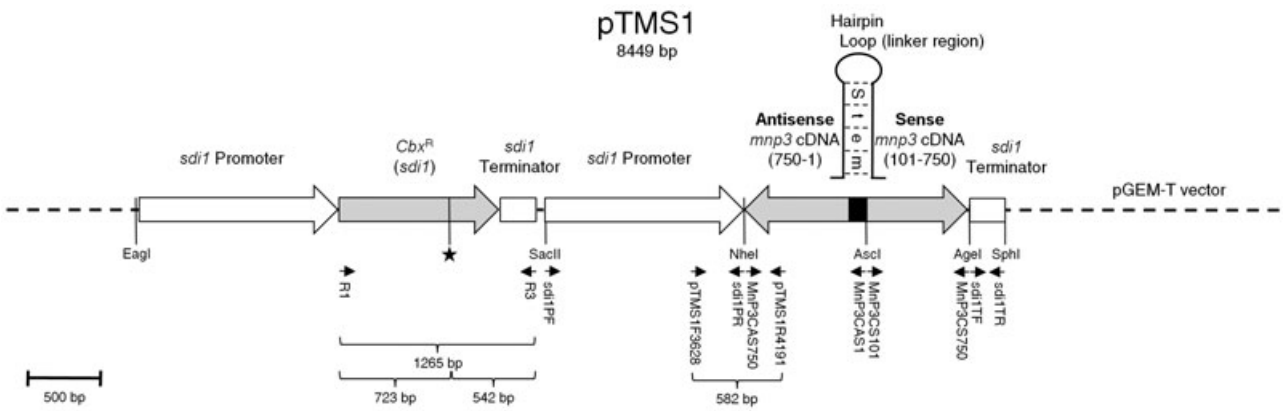

Fig. 3. Map of the *P. ostreatus* PC9 *mnp3* RNAi induction and carboxin resistance conferring plasmid pTMS1. The 750–1 bp and 101–750 bp fragments of *mnp3* cDNA were ligated in inverted orientation at the multiple cloning site of the vector pTM1, under the control of the *sdi1* promoter and terminator. The predicted transcribed hpRNA structure is illustrated. *Cbx*R, the mutant *sdi1* gene conferring resistance to carboxin. The asterisk '*' indicates unique SphI recognition site in the PC9 *sdi1* allele, which is not present in *Cbx*R. The location of the coding sequence and the direction of transcription are indicated by large arrows. The pGEM-T vector is marked by dashed lines. Small arrows indicate the location of the primers used for construction and detection of the construct.

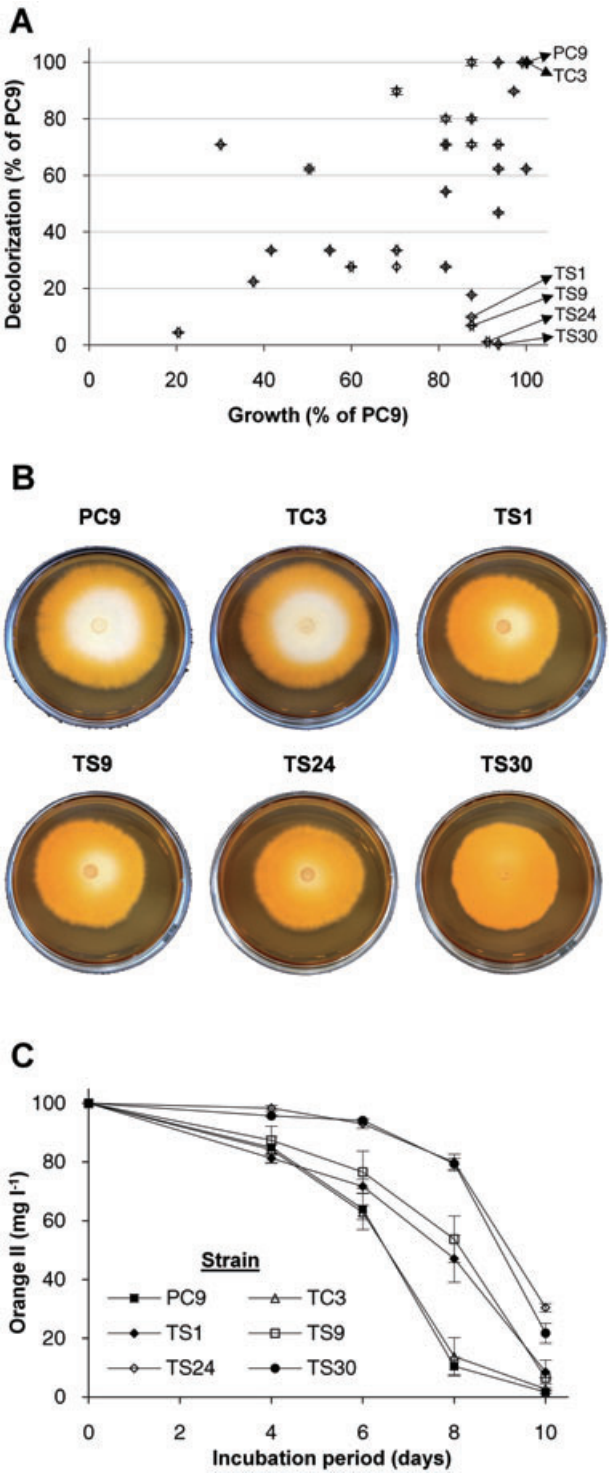

Fig. 4. A. Orange II decolourization and growth of *P. ostreatus* PC9 transformant strains in solid GP medium, amended with 27 μM Mn^{2+}, after 10 days of incubation. The markers (◇) represent growth versus decolourization area of the transformants, expressed as relative percent of PC9 (wild-type) values. Arrows indicate the strains selected for further examination. Data represent the average of three biological replicates. Bars denote the standard deviation.
B. Orange II decolourization by *P. ostreatus* PC9 strains in solid GP medium amended with 27 μM Mn^{2+}, after 10 days of incubation. PC9 – wild-type; TC3 – control strain (pTM1 transformant); TS1, TS9, TS24, TS30 – Mn^{2+}-dependent peroxidase silenced strains (pTMS1 transformants).
C. Time-course assay of Orange II decolourization by *P. ostreatus* PC9 and selected transformant strains in liquid culture of GP media, amended with 27 μM Mn^{2+}, during 10 days of incubation. Data represent the average of three biological replicates. Bars denote the standard deviation.

stable as they remained resistant to carboxin after three transfers in medium lacking the fungicide.

In order to determine whether pTMS1 transformants were affected in their ability to decolourize OII, the different strains were grown on solid GP medium containing OII, amended with 27 μM of Mn^{2+}, under carboxin selection pressure. Growth and decolourization, after 10 days of incubation, were monitored and compared with the untransformed wild-type strain PC9 (Fig. 4A). TC3 exhibited similar growth (±3%) and decolourization (±5%) rates as PC9. pTMS1 transformants showed marked variability in their growth and OII decolourization capabilities. Of these, four strains, designated TS1, TS9, TS24 and TS30, which grew similarly to the wild-type (88–94%), but showed high inhibition (90–99%) in their OII decolourization capacity in comparison to PC9 and TC3, were selected for further examination (Fig. 4B).

OII decolourization by the four selected strains was measured in liquid GP medium amended with 27 μM Mn^{2+} for 10 days (Fig. 4C). The control strain, TC3, exhibited similar decolourization levels as the PC9 wild-type strain throughout the experiment. In contradiction, during the first 8 days of incubation, the pTMS1 transformants (TS1, TS9, TS24 and TS30) exhibited a significant lower rate of OII decolourization (albeit, at different levels). After this period extensive decolourization was observed in all strains. All the tested strains produced a similar biomass (239 ± 24 mg/flask) over the mentioned time period. Based on these results, which were consistent in both solid and liquid cultures, it can be concluded that Mn^{2+}-dependent peroxidase expression is indeed reduced in the examined strains, as a consequence of the genetic manipulation performed.

A control experiment was conducted to examine the effect of Mn^{2+} on the ability of the MnP silenced transformants to decolourize the anthraquinone dye Acid blue 62, whose decolourization by *P. ostreatus* has been attributed to laccase (Faraco *et al.*, 2009). We found that decolourization of acid blue 62 was independent of Mn^{2+} amendments, and both wild-type *P. ostreatus* and the transformants decolourized the dye similarly, with or without Mn^{2+} (Supporting Information; Fig. S1). This is in agreement with our conclusion that the inhibition of OII decolourization by the pTMS1 transformants is indeed due to specific silencing of Mn^{2+}-dependent peroxidases genes.

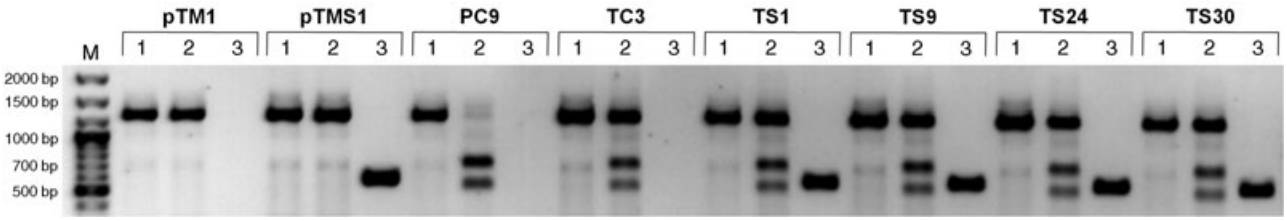

Fig. 5. PCR and restriction enzyme-based detection of the transformation construct DNA in transformant strains. Source of template DNA is indicated above the gel wells. Samples are: lane 1 – PCR amplicon of *sdi1* (*Cbx*^{R}); lane 2 – SphI digestion of the *sdi1* amplicon (SphI restriction site is present only in the endogenous PC9 *sdi1* allele, and not present in *Cbx*^{R} (a point-mutated *sdi1* allele of *P. ostreatus* strain #261-22); lane 3 – PCR amplicon of a segment corresponding to the *sdi1* promoter linked to the *mnp3* cDNA antisense (present only in the pTMS1 construct); M – DNA size marker [GeneRuler 100 bp Plus (Fermentas)].

To further verify the link between the transformation procedure and the phenotypic effects observed, we confirmed that the transformants analysed did, in fact, harbour the RNAi insert. Our analysis was based on the fact that carboxin resistance (*Cbx*^{R}) is conferred by a point-mutated *P. ostreatus sdi1* gene, whose source is an allelic *sdi1* fragment from *P. ostreatus* strain #261-22 (Irie *et al.*, 1998a; Honda *et al.*, 2000; GenBank AB009845). Analysis of the PC9 *sdi1* allele (This study; GenBank FJ598647) revealed a single-nucleotide alteration, which results in the presence of a unique SphI recognition site at position 724 bp in the PC9 *sdi1* allele, which is not present in the *Cbx*^{R}-resistance-conferring allele of *sdi1* (Fig. 3, marked by '*'). Accordingly, confirmation of the integrative nature of the constructs used was performed by PCR-based amplification of *sdi* gene fragment(s) followed by SphI-digestion, in order to confirm the presence of the *Cbx*^{R} gene; and a segment corresponding to the *sdi1* promoter linked to the *mnp3* cDNA antisense, in order to confirm the presence of the hpRNA expressing *mnp3* silencing construct (Fig. 3). On the basis of the resulting amplicons and SphI restriction profile (Fig. 5), the presence of the hpRNA expressing *mnp3* silencing construct in the relevant transformants was confirmed (For further explanation see Supporting Information).

MnP gene family expression is altered in strains harbouring mnp3 RNAi constructs

In order to determine whether alterations in MnP gene family transcript levels accompany the changes observed in OII decolourization we used relative real-time PCR quantification analysis. The selected strains (TS1, TS9, TS24, TS30 and the TC3 control) were grown for 7 days in liquid culture, in the presence of carboxin, in either a medium amended with 27 μM Mn^{2+} (+Mn treatment) or a non-amended medium (–Mn treatment). The results presented in Fig. 6 show the relative expression of the nine different members of the MnP gene family in the five selected strains. The overall abundance of the endogenous control gene (β-tubulin) transcript was found to be similar in all the strains in all the tested treatments. As TC3 exhibited similar gene expression levels to the PC9 wild-type strain, we used the former, in the –Mn treatment, as our calibrators for relative quantifications. The results obtained (Fig. 6) indicate that the predominantly expressed MnP gene family members expression in the pTMS1 transformants varied in intensity in response to Mn^{2+} amendment, similarly to the calibrator (TC3) and PC9 (Fig. 2), but at different levels. Specifically, relatively to the calibrator, *mnp3* and *mnp9* gene expression, though not substantially affected in the –Mn treatment (less than twofold difference), were strongly inhibited in the +Mn treatment which exhibited 24- to 79-fold higher levels in the calibrator. Therefore, *mnp3* and *mnp9* were not even remotely upregulated at levels comparable to the control in response to Mn^{2+} amendment. *mnp4* gene expression was not substantially affected in the –Mn treatment (less than 2.2-fold difference); however, in the +Mn treatment it was 8- to 24-fold higher in the calibrator; *mnp8* gene expression was not substantially affected in the –Mn treatment (less than 2 fold difference), but in the +Mn treatment it was 4- to 9-fold higher in the calibrator. Thus, in contrast to the striking results obtained in the case of *mnp3*, *4* and 9, the transcript abundance of *mnp1*, *2*, *5*, *6* and *7* was not substantially affected (less than fourfold difference), generally showing the same trend as the calibrator both in the –Mn and +Mn treatments.

In an attempt to explain the 'off-target' effects of the *mnp3* silencing construct on the other MnP gene family members, a Smith-Waterman local alignment of the silencing construct against the various *mnp*s transcripts was performed. The sequences were found to have potential cross-hybridization RNA fragments, according to the basic rules set by Yamada and Morishita (2005), thus providing a probable explanation for the silencing of other gene family members.

These results verify that transformation of *P. ostreatus* with an *mnp3* cDNA hpRNA expressing construct (pTMS1) induces strong silencing of the two Mn^{2+}-

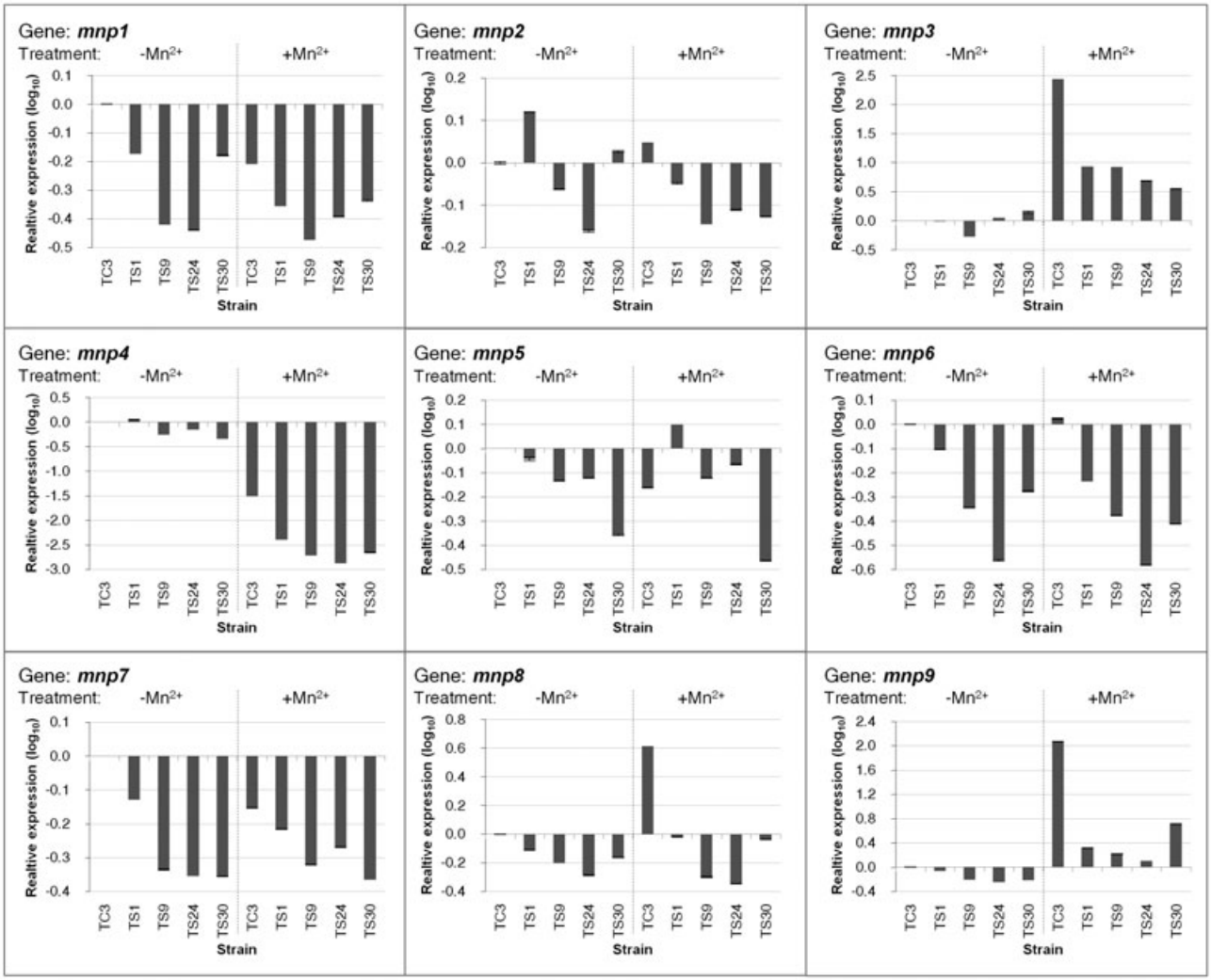

Fig. 6. Relative transcript abundance of MnP gene family members in RNA extracted from *P. ostreatus* PC9 transformants grown for 7 days in liquid GP medium amended with 27 μM Mn^{2+} (+Mn treatment), compared with that of the TC3 strain grown in non-amended medium (–Mn treatment). The abundance of *mnp1–9* genes transcripts, relative to β-tubulin, was measured by real-time PCR, and quantified by the ΔΔCT method. TC3 – control strain (pTM1 transformant); TS1, TS9, TS24, TS30 – Mn^{2+}-dependent peroxidase silenced strains (pTMS1 transformants). Data represent the average of three biological replicates. Bars denote the standard deviation; when not visible, the standard deviation is included within the graph line width. Note the $\log_{10}$ scale, and different axis ranges.

dependent peroxidase genes, *mnp3* and *mnp9*, and increases the reduction in *mnp4* transcript in the +Mn treatment, without substantially affecting the expression of the other MnP gene family members. Moreover, the silencing level of the *mnp3* gene (Fig. 6) strongly correlates with the level of inhibition in OII decolourization capacity of these strains both on solid and in liquid media (Fig. 4A and 4C respectively). The combined results from analysing the fungal response to Mn^{2+} amendments, as expressed by OII decolourization capacity, along with the changes in MnP gene family expression levels, support our conclusion linking the phenotypic effects observed with MnP gene silencing.

Discussion

Biodegradation of recalcitrant synthetic dyes by WRF and their enzymes has been extensively investigated during the last three decades. This property is attributed to the activity of the LMEs produced by these fungi which, due to their low substrate specificity, are capable of degrading a wide range of natural and xenobiotic aromatic compounds. Due to the structural similarity of these dyes to lignin (sub)structures, they are considered as model compounds for evaluation of the functionality of the fungal ligninolytic system (Glenn and Gold, 1983; Platt *et al.*, 1985; Field *et al.*, 1993; Knapp *et al.*, 1997; Cohen *et al.*,

2002a; Mielgo *et al*., 2003; Wesenberg *et al*., 2003; López *et al*., 2004; Shrivastava *et al*., 2005; Tsukihara *et al*., 2006; Asgher *et al*., 2008; Hernández-Luna *et al*., 2008; Faraco *et al*., 2009; Stajić *et al*., 2009). Decolourization of some dyes, such as Acid blue 62, has been attributed to laccase activity (Faraco *et al*., 2009), whereas that of others, such as OII, has been shown to be dependent on the presence of Mn^{2+}, suggesting the involvement of Mn^{2+}-peroxidases (Knapp *et al*., 1997; Mielgo *et al*., 2003; López *et al*., 2004). Indeed, in the current study, we have also witnessed the differential dependence of Acid blue 62 and OII degradation on Mn^{2+} amendment.

Previous studies demonstrated that Mn^{2+} amendment greatly enhances the ligninolytic degradative capabilities of *P. ostreatus*. This was presumably due to an increase in the activity and transcript levels of Mn^{2+}-dependent peroxidase (Camarero *et al*., 1996; Kerem and Hadar, 1997; Cohen *et al*., 2001; 2002b). Similarly, MnP expression in *Phanerochaete chrysosporium* was shown to be positively regulated by Mn^{2+} (Gettemy *et al*., 1998; Kersten and Cullen, 2007). To evaluate the molecular genetic basis for the enhanced decolourization of OII in the presence of Mn^{2+}, we identified the components of the *P. ostreatus* MnP gene family and followed their transcription profile.

Prior to this study, only four known members of this gene family (*mnp1–4*) have been studied (see Table 1). Annotation of the recently sequenced *P. ostreatus* genome revealed that this gene family is comprised of at least nine members, five of which (*mnp5–9*) have not been previously studied (Table 1; http://genome.jgi-psf.org/PleosPC15-1). Due to the fact that these genes were found to be closely related, the use of specific primers, designed on the basis of non-conserved regions, was required to study their transcription profile. Our results confirm that all nine genes (*mnp1–9*) are transcribed, and that Mn^{2+} differentially regulates the abundance of the MnPs (*mnp3* and *mnp9*) and VP (*mnp4*) transcripts, all of which have a substantially higher level of basal transcript abundance than the other family members. In Mn^{2+}-containing cultures the transcript levels of *mnp3* and *mnp9* were drastically increased relative to the non-amended medium, and a concomitant marked reduction in *mnp4* transcript abundance was measured (Fig. 2). *mnp3* encodes a Mn^{2+}-dependent peroxidase, and the deduced amino acid sequence of *mnp9* indicates that this gene also encodes a Mn^{2+}-dependent peroxidase, whereas *mnp4* is known to encode a VP (Asada *et al*., 1995; Ruiz-Dueñas *et al*., 1999; Giardina *et al*., 2000; Irie *et al*., 2000; Cohen *et al*., 2001; http://genome.jgi-psf.org/PleosPC15-1).

Multiple LME isoenzymes, encoded by various, and apparently redundant structurally related genes, is common among wood-associated fungi. For example, *P. chrysosporium*, *Ceriporiopsis subvermispora* and *Phlebia chry*socreas have at least 5, 4 and 7 different genes encoding MnPs respectively (Kersten and Cullen, 2007; Gutiérrez *et al*., 2008; Morgenstern *et al*., 2008), while *P. ostreatus*, *Coprinopsis cinerea* and *Laccaria bicolor* have at least 7, 17 and 11 different genes encoding laccases respectively (Kilaru *et al*., 2006; Courty *et al*., 2009; Pezzella *et al*., 2009). Studies of the catalytic properties of various LME isoenzymes reflected distinct differences in both the culture conditions and substrate specificity associated with their transcription and kinetic constants. For example, seven isoforms of MnPs were isolated from *C. subvermispora* cultures in salt medium, whereas four isoenzymes were fractioned in extracts derived from wood chips. The requirement for Mn^{2+} by each of these MnPs varied on the basis of the nature of the aromatic substrate (vanillylacetone, *o*-dianisidine, *p*-dianisidine, guaiacol) added to the reaction mixture (Urzúa *et al*., 1995). *Phanerochaete chrysosporium* MnP gene expression is regulated by nitrogen levels, Mn^{2+} as well as by heat shock, agitation and other factors. While *mnp1–3* are expressed under various culture conditions, *mnp4* and *mnp5* seem to be actively transcribed only when the fungus is grown on wood-containing soil samples, and wood pulp respectively (Gettemy *et al*., 1998; Kersten and Cullen, 2007).

The fact the *P. ostreatus* has a large number of distinct genes encoding transcripts of various isoenzymes belonging to the MnP gene family points to the potential redundancy and/or diversity of these enzymes, and may imply that complex and versatile strategies are employed by this fungus for the degradation of aromatic and recalcitrant compounds such as amorphic lignin and azo dyes. Moreover, these enzymes were shown to be differentially regulated by Mn^{2+}, and it is also probable that they may prove to have different substrate specificity and catalytic properties.

The recent introduction of a DNA-mediated transformation procedure of *Pleurotus* provides a platform for utilizing genetic-based strategies for gene function analyses (Honda *et al*., 2000; Irie *et al*., 2001b). Gene overexpression was used to study the elevated expression of *mnp2* and *mnp3* (Irie *et al*., 2001a; Tsukihara *et al*., 2006). MnP2 was further characterized by site-directed mutagenesis (Tsukihara *et al*., 2008).

RNAi has been proven effective for gene expression downregulation in most eukaryotes, including vertebrates, plants, worms, protists and fungi (Nakayashiki and Nguyen, 2008). This method has proven especially useful when homologous recombination, necessary for gene targeting using knockout techniques, occurs at low frequency (Matityahu *et al*., 2008; Nakayashiki and Nguyen, 2008; Kemppainen *et al*., 2009), such as in the predominant random ectopic integration of transformed

DNA into *Pleurotus* (Honda *et al.*, 2000; Irie *et al.*, 2001a). Furthermore, unlike conventional gene disruption methods, RNAi confers only partial reduction (knock-down) but not complete loss (knockout) of gene expression. The incomplete gene suppression frequently results in phenotypic variations that may provide more detailed information concerning the function of the silenced gene (Nakayashiki and Nguyen, 2008). Within the framework of the *P. ostreatus* genome deciphering project, our preliminary results identified genes encoding orthologues of key components of the RNA-mediated gene silencing machinery (Argonaute, Dicer and RdRP) (Tomari and Zamore, 2005; Nakayashiki *et al.*, 2006; Nakayashiki and Nguyen, 2008), supporting the feasibility of RNAi-mediated gene expression regulation in this fungus (expressed sequence tags have also been found for many of these genes) (http://genome.jgi-psf.org/PleosPC15-1). We therefore employed an RNAi-based approach for gene knock-down of Mn^{2+}-dependent peroxidases, followed by evaluation of OII decolourization and MnP gene family transcription abundance levels in the corresponding strains, demonstrating that the expression of Mn^{2+}-dependent peroxidases can be directly associated with *P. ostreatus* ligninolytic degradative capabilities. Since the data regarding the existence of *mnp5–9* were not available until the final stages of this project, our strategy focused on targeting *mnp3*, which was the only gene known to encode for Mn^{2+}-dependent peroxidase in *P. ostreatus* at the time.

To date, plasmid constructs expressing hpRNA or intron containing hpRNA are the most prevalent and reliable platforms to induce RNAi in fungi. These types of vectors have been successfully used to demonstrate RNAi using model genes and to explore gene function in a wide range of fungal species. In filamentous fungi specifically, this strategy has been shown to induce the most efficient, systemic, *trans*-acting and stable silencing (Nakayashiki and Nguyen, 2008). With this in mind, pTMS1, the vector designed to induce RNAi-based gene silencing of *mnp3*, was constructed according to the basic principle of expressing an hpRNA.

Another advantage of RNAi, is that, in contrast to the gene knockout approach, it facilitates a *trans*-acting effect of reducing gene expression in the transformed strains without having the need for mating, production of fruiting bodies and spores, for isolation of transformant monokaryons, in order to obtain observable silencing effects, which may have been necessary using knockout techniques (Nakayashiki and Nguyen, 2008). In this respect, silencing via RNAi can result in the simultaneous suppression of expression of an entire gene family, thus avoiding compensatory effects of redundant gene family members. Simultaneous interference with homologous family members by using dsRNA has been demonstrated in trypanosomes and *Drosophila*. In fact, in most protozoan parasites and fungi, this approach is significantly more efficient than constructing multiple knockout strains (Nakayashiki and Nguyen, 2008).

These characteristic RNAi effects could be clearly seen in strains harbouring *mnp3* RNAi constructs. Integration of the *mnp3*-silencing cassette caused a substantial reduction in both the expression levels of *mnp3*, *9* and *4* and in OII decolourization capacity (Figs 4 and 6). Nonetheless, and even though *sdi1* expression signals are considered to be constitutive (Irie *et al.*, 1998b; 2001a,b; Honda *et al.*, 2000; Tsukihara *et al.*, 2006), both effects were not total, as the silenced strains still exhibited decolourization, pronounced in the late stages of incubation. This phenomenon is most likely due to the incomplete suppression of the expression of the MnP genes, which allowed gradual accumulation of MnPs to sufficient levels for decolourization. Indeed, the silencing level of the *mnp3* gene positively correlated with the level of inhibition of OII decolourization capacity of these strains (Figs 4 and 6). Similar 'off-target effects' were described by Matityahu *et al.* 2008 when attempting to silence the *P. chrysosporium MnSOD1* gene. There, the *MnSOD1* RNAi construct also indirectly led to the partial silencing of *MnSOD2* and *3*, two other genes that belong to the *MnSOD* gene family.

In this study, the outcome of our attempt to silence *mnp3* clearly illustrates the potential multigene silencing capacity of RNAi (Fig. 6). These effects can be attributed to the nature of the hpRNA construct we employed (Fig. 3), which contained numerous regions that are highly conserved among various members of the MnP gene family. Due to this sequence similarity, and as may be expected, the homologous nontargeted members of this multiple gene family were simultaneously silenced, along with the 'true target' – *mnp3*. This phenomenon may have been to our advantage, since it resulted in silencing of *mnp9*, in addition to *mnp3* (Fig. 6). Whether or not *mnp9* and *mnp3* truly have redundant or compensatory functions has yet to be determined.

Taken together, we established the first direct association between Mn^{2+}-dependent peroxidases (*mnp3* and *mnp9*) level of gene expression and azo dye decolourization capacity in *P. ostreatus*. This conclusion was obtained here on the basis of an RNAi reverse genetics approach, now providing a proven platform for further dissection of gene family function in *P. ostreatus*.

Lastly, to date, most of the insight obtained on the mechanism of lignin degradation by *P. ostreatus* has been based on biochemical and physiological analyses (Camarero *et al.*, 1996; Kerem and Hadar, 1997; Cohen *et al.*, 2001; 2002b). The current study advances our understanding of the genetic basis of these mechanisms.

Experimental procedures

Fungal and bacterial strains and growth conditions

Pleurotus ostreatus monokaryon strain PC9 (Spanish Type Culture Collection accession number CECT20311), which is a protoclone derived by dedikaryotization of the dikaryon commercial strain N001 (Larraya *et al.*, 1999), was used throughout this study. Fungal strains were grown and maintained in YMG medium [1% w/v glucose, 1% w/v malt extract (Difco), 0.4% w/v yeast extract (Difco)] (Irie *et al.*, 2001b) or in GP medium [2% w/v glucose, 0.5% w/v peptone (Difco), 0.2% w/v yeast extract (Difco), 0.1% w/v K_2HPO_4, 0.05% w/v $MgSO_4{\cdot}7H_2O$] (Irie *et al.*, 2001a); Mn^{2+} was added as $MnSO_4$ as specified. Solid culture was performed in 9 cm diameter Petri dishes containing 15 ml media solidified with 1.5% w/v agar. Liquid cultures were maintained in stationary 100 ml Erlenmeyer flasks containing 10 ml media. Cultures were incubated at 28°C in the dark. The inoculum for all growth conditions was one disk (5 mm diameter) of mycelium, from the edge of a freshly grown colony in solid culture, positioned at the centre of the Petri dish or the flask. The azo dye Orange II [4-(2-hydroxy-1-naphthylazo)benzenesulfonic acid sodium salt] and the fungicide carboxin (Sigma-Aldrich) were added to a final concentration of 100 mg l^{-1} and 8.5 μM (LD_{50} = 0.7 μM), respectively, as specified. Mycelial growth in solid culture was evaluated by measuring colony area, and in liquid culture biomass production was measured as dry weight (oven dried to constant weight at 65°C). *Escherichia coli* JM109 cells (Invitrogen) were used for standard cloning procedures according to the manufacturer's protocol.

Analysis of Orange II decolourization

In solid culture, OII decolourization capacity was estimated according to the visually decolourized area, as measured from the centre of the inoculation point. In liquid culture, 200 μl of the media was centrifuged (4720 *g*, 10 min, room temperature) and mixed with 800 μl phosphate buffer (0.1 M, pH 7.0). OII dye concentration in the media was quantified according to the absorption reading of the solution at λ_{max} 483 nm, using a BioMate 3 spectrophotometer (Thermo Spectronic), according to a standard curve. Non-inoculated medium amended with OII was used as a control.

Nucleic acid manipulation and analysis

Molecular manipulations were carried out on the basis of standard protocols (Sambrook *et al.*, 1989). Commercial kits were used according to the manufacturer's instructions. Genomic DNA was isolated using the ZR Fungal/Bacterial DNA Kit (Zymo Research). RNA was extracted from 7-day-old cultures, grown in liquid GP medium, either non-amended or amended with 27 μM of Mn^{2+}, using the RNeasy Plant Mini Kit (Qiagen) along with the manufacturer's RLC lysis buffer. cDNA synthesis was performed using the SuperScript III First-Strand Synthesis System for RT-PCR (Invitrogen). Plasmid DNA purification was performed using the QIAprep Spin Miniprep Kit (Qiagen). PCR was performed on an Eppendorf Mastercycler Gradient Thermocycler (Eppendorf), using BIO-X-ACT Short Mix (BIOLINE), with the primers detailed in Table 1. DNA endonuclease restriction and ligation were performed using restriction enzymes and T4 DNA Ligase from Fermentas. Isolation and purification of DNA fragments from agarose gel or PCR amplification was performed using the kit Wizard SV Gel and PCR Clean-Up System (Promega). Cloning to plasmids was performed using the kit pGEM-T Vector System II (Promega). Full sequencing was performed for all the DNA fragments, plasmids and real-time PCR amplicons, in the Center for Genomic Technologies at the Hebrew University of Jerusalem. Real-time PCR relative quantification analysis by the ΔΔCT method (Livak and Schmittgen, 2001) was performed on an ABI Prism 7000 Sequence Detection System and software (Applied Biosystems), using SYBR Green PCR Master Mix (Applied Biosystems), with the primers detailed in Table 1 and an annealing temperature of 63°C, according to the manufacturer's default operating procedures.

Construction of pTMS1: an mnp3 silencing vector

The construct for RNAi silencing of *mnp3* was designed with inverted 650 bp repeats, corresponding to the first 650 bp of *mnp3* cDNA (This study; GenBank FJ594281), separated by a 100 bp loop (linker region) corresponding to *mnp3* cDNA 100–1 bp, under the control of *sdi1* expression signals, which was ligated into the pTM1 plasmid (Honda *et al.*, 2000), harbouring the carboxin resistance gene, Cbx^R, under the control of *sdi1* expression signals; the resulting plasmid was designated pTMS1 (Fig. 3; see also *Results*). All the primers used in the construction procedure are listed in Table 1 and indicated in Fig. 3; these primers were designed with unique restriction sites at their ends, to facilitate directional cloning of the corresponding fragments. Specifically, *mnp3* cDNA was amplified using primers MnP3C1 and MnP3C2. *sdi1* promoter was amplified from pTM1 using primers sdi1PF and Sdi1PR, which adapts the restriction sites SacII and NheI respectively. The antisense (+linker region) segment, corresponding to *mnp3* cDNA 750–1 bp, was amplified from *mnp3* cDNA using primers MnP3CAS750 and MnP3CAS1, which adapts the restriction sites NheII and AscI respectively. The sense segment, corresponding to *mnp3* cDNA 101–750 bp, was amplified from *mnp3* cDNA using primers MnP3CS101 and MnP3CS750, which adapts the restriction sites AscI and AgeI respectively. *sdi1* terminator was amplified from pTM1 using primers sdi1TF and Sdi1TR, which adapts the restriction sites AgeI and SphI respectively. Each of the amplified segments was separately cloned into a pGEM-T vector (Promega). The promoter, antisense (+linker region), sense and terminator segments were then extracted via endonuclease digestion with the corresponding restriction enzymes specified above; and plasmid pTM1 was digested with the restriction enzymes SphI and SacII. All the digested segments were isolated and purified from agarose gel, and then mixed together in a ligation reaction. The resulting ligation mixture was transformed into *E. coli* using the pGEM-T Vector System II (Promega); and plasmids were successively purified and screened via digestion to locate the desired plasmid. This plasmid was designated pTMS1 (Fig. 3) and it was entirely sequenced to confirm that all the segments were cloned correctly (both in location and orientation).

Fungal transformation

Transformation was performed based on the PEG/$CaCl_2$ protocol previously adapted for *P. ostreatus* (Honda *et al*., 2000; Irie *et al*., 2001b). The fungicide carboxin was used as a selective marker, and conferring resistance was achieved via introduction of the carboxin-resistance marker gene, *Cbx*^{R}, which was constructed by introducing a base substitution in the *sdi1* gene (allele of strain #261-22) coding sequence (Honda *et al*., 2000). Competent protoplasts were produced by digestion of *P. ostreatus* mycelium, from liquid culture in YMG medium, with lytic enzymes. The lytic enzymes solution was comprised of 2% w/v Lysing enzymes from *Trichoderma harzianum* (Sigma-Aldrich) and 0.2% w/v Chitinase from *Trichoderma viride* (Sigma-Aldrich), in 0.5% w/v sucrose as an osmotic stabilizer. The protoplasts were washed in STC solution (18.2% w/v sorbitol, 50 mM $CaCl_2$, 50 mM Tris-HCl pH 8.0, 0.5 M sucrose), and adjusted to a final concentration of 5×10^7 protoplasts ml^{-1}. Then 200 μl of protoplasts were mixed with 10 μl of plasmid DNA (200 ng μl^{-1}), 30 μl of single-strand λ phage carrier DNA (500 μg ml^{-1}, after denaturation at 95°C for 5 min and immediate transfer to ice), and 15 μl of heparin (5 mg dissolved in 1 ml of STC solution). After 40 min of incubation on ice, 1 ml of PTC solution (40% w/v PEG#4000, 50 mM $CaCl_2$, 50 mM Tris-HCl pH 8.0, 0.5 M sucrose) was added, and the mixture was incubated for 20 min at room temperature. The mixture was then plated on selective YMG solid regeneration medium, containing 0.5 M sucrose and carboxin at a final concentration of 8.5 μM. Transformants were isolated after 10 days of incubation at 28°C. The transformants stability was verified by three successive transfers (inoculated from the edge of a 7-day-old colony) to solid medium without carboxin, and then returning and maintaining them in selective solid culture amended with carboxin.

Screening and evaluation of P. ostreatus *Mn^{2+}-dependent peroxidase silenced transformants*

Thirty pTMS1 transformants were isolated, alongside one randomly chosen control strain (TC3) transformed with pTM1. These transformants were analysed for both phenotypic and genotypic properties. Phenotypic analysis was performed in three stages: (i) selection of strains growing on solid medium under carboxin selection pressure; (ii) evaluation of their OII decolourization capacity on solid medium (which allowed for a large scale screen), followed by selection of strains exhibiting similar growth but high inhibition of their OII decolourization capability compared with the wild-type (Fig. 4A and 4B); and (iii) quantitative time-course assay of OII decolourization and biomass production by the selected strains in liquid culture (Fig. 4C). Genotypic analysis was performed at two levels: (i) confirmation of the constructs integration into the selected strains genome, by isolation of genomic DNA which served for specific PCR detection of the *Cbx*^{R} (*sdi1*) gene, using primers R1 and R3, followed by SphI-digestion, in order to confirm the presence of the *Cbx*^{R} gene; and a segment corresponding to the *sdi1* promoter linked to the *mnp3* cDNA antisense, using primers pTMS1F3628 and pTMS1R4191, to confirm the presence of the hpRNA *mnp3* silencing construct (Table 1; Figs 3 and 5; see *Results* and Supporting Information for more details); (ii) evaluation of MnP gene family expression levels by extraction of RNA from liquid cultures of the selected strains, either non-amended or amended with 27 μM Mn^{2+}, followed by relative real-time PCR quantification analysis, in order to confirm silencing effects of Mn^{2+}-dependent peroxidases gene expression (Table 1 and Fig. 6).

Acknowledgements

We are deeply grateful to Professor Takashi Watanabe and Professor Yoichi Honda, Research Institute for Sustainable Humanosphere, Kyoto University, Japan, for generously providing plasmid pTM1. We also thank the Joint Genome Institute (US Department of Energy) and the *Pleurotus* Genome Consortium for access to the *P. ostreatus* genome sequence prior to publication. This work was supported in part by the Joint Israeli-Lower Saxony research projects financed by the Lower Saxony Ministry of Science and Culture.

References

Asada, Y., Watanabe, A., Irie, T., Nakayama, T., and Kuwahara, M. (1995) Structures of genomic and complementary DNAs coding for *Pleurotus ostreatus* manganese(II) peroxidase. *BBA-Protein Struct M* **1251:** 205–209.

Asgher, M., Bhatti, H.N., Ashraf, M., and Legge, R.L. (2008) Recent developments in biodegradation of industrial pollutants by white rot fungi and their enzyme system. *Biodegradation* **19:** 771–783.

Camarero, S., Böckle, B., Martínez, M.J., and Martínez, A.T. (1996) Manganese-mediated lignin degradation by *Pleurotus pulmonarius*. *Appl Environ Microbiol* **62:** 1070–1072.

Camarero, S., Sarkar, S., Ruiz-Dueñas, F.J., Martínez, M.J., and Martínez, A.T. (1999) Description of a versatile peroxidase involved in the natural degradation of lignin that has both manganese peroxidase and lignin peroxidase substrate interaction sites. *J Biol Chem* **274:** 10324–10330.

Cohen, R., Hadar, Y., and Yarden, O. (2001) Transcript and activity levels of different *Pleurotus ostreatus* peroxidases are differentially affected by Mn^{2+}. *Environ Microbiol* **3:** 312–322.

Cohen, R., Persky, L., and Hadar, Y. (2002a) Biotechnological applications and potential of wood-degrading mushrooms of the genus *Pleurotus*. *Appl Microbiol Biotechnol* **58:** 582–594.

Cohen, R., Persky, L., Hazan-Eitan, Z., Yarden, O., and Hadar, Y. (2002b) Mn^{2+} alters peroxidase profiles and lignin degradation by the white-rot fungus *Pleurotus ostreatus* under different nutritional and growth conditions. *Appl Biochem Biotechnol* **102:** 415–429.

Courty, P.E., Hoegger, P.J., Kilaru, S., Kohler, A., Buée, M., Garbaye, J., *et al.* (2009) Phylogenetic analysis, genomic organization, and expression analysis of multi-copper oxidases in the ectomycorrhizal basidiomycete *Laccaria bicolor*. *New Phytol* **182:** 736–750.

Faraco, V., Pezzella, C., Miele, A., Giardina, P., and Sannia, G. (2009) Bio-remediation of colored industrial wastewaters by the white-rot fungi *Phanerochaete chrysosporium* and *Pleurotus ostreatus* and their enzymes. *Biodegradation* **20:** 209–220.

Field, J.A., de Jong, E., Feijoo-Costa, G., and de Bont, J.A.M. (1993) Screening for ligninolytic fungi applicable to the biodegradation of xenobiotics. *Trends Biotechnol* **11:** 44–49.

Gettemy, J.M., Ma, B., Alic, M., and Gold, M.H. (1998) Reverse transcription-PCR analysis of the regulation of the manganese peroxidase gene family. *Appl Environ Microbiol* **64:** 569–574.

Giardina, P., Palmieri, G., Fontanella, B., Rivieccio, V., and Sannia, G. (2000) Manganese peroxidase isoenzymes produced by *Pleurotus ostreatus* grown on wood sawdust. *Arch Biochem Biophys* **376:** 171–179.

Glenn, J.K., and Gold, M.H. (1983) Decolorization of several polymeric dyes by the lignin-degrading basidiomycete *Phanerochaete chrysosporium*. *Appl Environ Microbiol* **45:** 1741–1747.

Gutiérrez, M., Rojas, L.A., Mancilla-Villalobos, R., Seelenfreund, D., Vicuña, R., and Lobos, S. (2008) Analysis of manganese-regulated gene expression in the ligninolytic basidiomycete *Ceriporiopsis subvermispora*. *Curr Genet* **54:** 163–173.

Hammel, K.E., and Cullen, D. (2008) Role of fungal peroxidases in biological ligninolysis. *Curr Opin Plant Biol* **11:** 349–355.

Hernández-Luna, C.E., Gutiérrez-Soto, G., and Salcedo-Martínez, S.M. (2008) Screening for decolorizing basidiomycetes in Mexico. *World J Microbiol Biotechnol* **24:** 465–473.

Hofrichter, M. (2002) Review: lignin conversion by manganese peroxidase (MnP). *Enzyme Microb Technol* **30:** 454–466.

Honda, Y., Matsuyama, T., Irie, T., Watanabe, T., and Kuwahara, M. (2000) Carboxin resistance transformation of the homobasidiomycete fungus *Pleurotus ostreatus*. *Curr Genet* **37:** 209–212.

Irie, T., Honda, Y., Matsuyama, T., Watanabe, T., and Kuwahara, M. (1998a) Cloning and characterization of the gene encoding the iron-sulfur protein of succinate dehydrogenase from *Pleurotus ostreatus*. *BBA-Gene Struct Expr* **1396:** 27–31.

Irie, T., Honda, Y., Matsuyama, T., Watanabe, T., and Kuwahara, M. (1998b) Isolation and sequence analysis of the promoter and an allelic sequence of the iron-sulfur protein subunit gene from the white-rot fungus *Pleurotus ostreatus*. *J Wood Sci* **44:** 491–494.

Irie, T., Honda, Y., Ha, H.C., Watanabe, T., and Kuwahara, M. (2000) Isolation of cDNA and genomic fragments encoding the major manganese peroxidase isozyme from the white rot basidiomycete *Pleurotus ostreatus*. *J Wood Sci* **46:** 230–233.

Irie, T., Honda, Y., Watanabe, T., and Kuwahara, M. (2001a) Homologous expression of recombinant manganese peroxidase genes in ligninolytic fungus *Pleurotus ostreatus*. *Appl Microbiol Biotechnol* **55:** 566–570.

Irie, T., Honda, Y., Watanabe, T., and Kuwahara, M. (2001b) Efficient transformation of filamentous fungus *Pleurotus ostreatus* using single-strand carrier DNA. *Appl Microbiol Biotechnol* **55:** 563–565.

Kemppainen, M., Duplessis, S., Martin, F., and Pardo, A.G. (2009) RNA silencing in the model mycorrhizal fungus *Laccaria bicolor*: gene knock-down of nitrate reductase results in inhibition of symbiosis with *Populus*. *Environ Microbiol* **11:** 1878–1896.

Kerem, Z., and Hadar, Y. (1997) The role of manganese in enhanced lignin degradation by *Pleurotus* ostreatus. In *TAPPI Proceedings, Biological Sciences Symposium*. Atlanta, GA, USA: TAPPI Press, pp. 29–33.

Kersten, P., and Cullen, D. (2007) Extracellular oxidative systems of the lignin-degrading basidiomycete *Phanerochaete chrysosporium*. *Fungal Genet Biol* **44:** 77–87.

Kilaru, S., Hoegger, P.J., and Kües, U. (2006) The laccase multi-gene family in *Coprinopsis cinerea* has seventeen different members that divide into two distinct subfamilies. *Curr Genet* **50:** 45–60.

Knapp, J.S., Newby, P.S., and Reece, L.P. (1995) Decolorization of dyes by wood-rotting basidiomycete fungi. *Enzyme Microb Technol* **17:** 664–668.

Knapp, J.S., Zhang, F.M., and Tapley, K.N. (1997) Decolourisation of Orange II by a wood-rotting fungus. *J Chem Technol Biotechnol* **69:** 289–296.

Larraya, L.M., Pérez, G., Peñas, M.M., Baars, J.J.P., Mikosch, T.S.P., Pisabarro, A.G., and Ramírez, L. (1999) Molecular karyotype of the white rot fungus *Pleurotus ostreatus*. *Appl Environ Microbiol* **65:** 3413–3417.

Livak, K.J., and Schmittgen, T.D. (2001) Analysis of relative gene expression data using real-time quantitative PCR and the $2^{-\Delta\Delta C_T}$ method. *Methods* **25:** 402–408.

López, C., Moreira, M.T., Feijoo, G., and Lema, J.M. (2004) Dye decolorization by manganese peroxidase in an enzymatic membrane bioreactor. *Biotechnol Progr* **20:** 74–81.

López, C., García-Monteagudo, J.C., Moreira, M.T., Feijoo, G., and Lema, J.M. (2007) Is the presence of dicarboxylic acids required in the MnP cycle? Study of Mn^{3+} stability by cyclic voltammetry. *Enzyme Microb Technol* **42:** 70–75.

Lucas, M., Mertens, V., Corbisier, A.M., and Vanhulle, S. (2008) Synthetic dyes decolourisation by white-rot fungi: Development of original microtitre plate method and screening. *Enzyme Microb Technol* **42:** 97–106.

Martínez, A.T. (2002) Molecular biology and structure-function of lignin-degrading heme peroxidases. *Enzyme Microb Technol* **30:** 425–444.

Matityahu, A., Hadar, Y., Dosoretz, C.G., and Belinky, P.A. (2008) Gene silencing by RNA interference in the white rot fungus *Phanerochaete chrysosporium*. *Appl Environ Microbiol* **74:** 5359–5365.

Mielgo, I., Moreira, M.T., Feijoo, G., and Lema, J.M. (2001) A packed-bed fungal bioreactor for the continuous decolourisation of azo-dyes (Orange II). *J Biotechnol* **89:** 99–106.

Mielgo, I., Lopez, C., Moreira, M.T., Feijoo, G., and Lema, J.M. (2003) Oxidative degradation of azo dyes by manganese peroxidase under optimized conditions. *Biotechnol Progr* **19:** 325–331.

Morgenstern, I., Klopman, S., and Hibbett, D.S. (2008) Molecular evolution and diversity of lignin degrading heme peroxidases in the agaricomycetes. *J Mol Evol* **66:** 243–257.

Nakayashiki, H., and Nguyen, Q.B. (2008) RNA interference: roles in fungal biology. *Curr Opin Microbiol* **11:** 494–502.

Nakayashiki, H., Kadotani, N., and Mayama, S. (2006) Evolution and diversification of RNA silencing proteins in fungi. *J Mol Evol* **63:** 127–135.

Pezzella, C., Autore, F., Giardina, P., Piscitelli, A., Sannia, G., and Faraco, V. (2009) The *Pleurotus ostreatus* laccase multi-gene family: isolation and heterologous expression of new family members. *Curr Genet* **55:** 45–57.

Platt, M.W., Hadar, Y., and Chet, I. (1985) The decolorization of the polymeric dye Poly-Blue (polyvinalamine sulfonate-anthroquinone) by lignin degrading fungi. *Appl Microbiol Biotechnol* **21:** 394–396.

Ruiz-Dueñas, F.J., Martínez, M.J., and Martínez, A.T. (1999) Molecular characterization of a novel peroxidase isolated from the ligninolytic fungus *Pleurotus eryngii*. *Mol Microbiol* **31:** 223–235.

Ruiz-Dueñas, F.J., Camarero, S., Pérez-Boada, M., Martínez, M.J., and Martínez, A.T. (2001) A new versatile peroxidase from *Pleurotus*. *Biochem Soc Trans* **29:** 116–122.

Sambrook, J., Fritsch, E.F., and Maniatis, T. (1989) *Molecular Cloning: A Laboratory Manual*. Cold Spring Harbor, NY, USA: Cold Spring Harbor Laboratory Press.

Shrivastava, R., Christian, V., and Vyas, B.R.M. (2005) Enzymatic decolorization of sulfonphthalein dyes. *Enzyme Microb Technol* **36:** 333–337.

Stajić, M., Vukojević, J., and Duletić-Laušević, S. (2009) Biology of *Pleurotus eryngii* and role in biotechnological processes: a review. *Crit Rev Biotechnol* **29:** 55–66.

Tomari, Y., and Zamore, P.D. (2005) Perspective: machines for RNAi. *Gene Dev* **19:** 517–529.

Tsukihara, T., Honda, Y., and Watanabe, T. (2006) Molecular breeding of white rot fungus *Pleurotus ostreatus* by homologous expression of its versatile peroxidase MnP2. *Appl Microbiol Biotechnol* **71:** 114–120.

Tsukihara, T., Honda, Y., Sakai, R., and Watanabe, T. (2008) Mechanism for oxidation of high-molecular-weight substrates by a fungal versatile peroxidase, MnP2. *Appl Environ Microbiol* **74:** 2873–2881.

Urzúa, U., Larrondo, L.F., Lobos, S., Larraín, J., and Vicuña, R. (1995) Oxidation reactions catalyzed by manganese peroxidase isoenzymes from *Ceriporiopsis subvermispora*. *FEBS Lett* **371:** 132–136.

Wesenberg, D., Kyriakides, I., and Agathos, S.N. (2003) White-rot fungi and their enzymes for the treatment of industrial dye effluents. *Biotechnol Adv* **22:** 161–187.

Yamada, T., and Morishita, S. (2005) Accelerated off-target search algorithm for siRNA. *Bioinformatics* **21:** 1316–1324.

Supporting information

Additional Supporting Information may be found in the online version of this article:

Fig. S1. Acid blue 62 decolourization by *P. ostreatus* strains grown in solid GP media containing several concentrations of Mn^{2+} (0–270 μM), after 10 days of incubation. PC9 – wild-type; TC3 – control strain (pTM1 transformant); TS1, TS9, TS24, TS30 – Mn^{2+}-dependent peroxidase silenced strains (pTMS1 transformants). The light and dark columns represent mycelial growth and the decolourized area respectively. Data represent the average of three biological replicates. Bars denote the standard deviation.

Please note: Wiley-Blackwell are not responsible for the content or functionality of any supporting materials supplied by the authors. Any queries (other than missing material) should be directed to the corresponding author for the article.

